Journal of Information Display, vol. 5, no. 1, 2004

Design and Analysis of Diffractive Grating Imprinted Light-guide Plate for LCD Illumination

Hwan Young Choi[a] and Young-Pil Park[b]

Abstract

A highly simplified backlight unit mainly composed of diffractive grating in sub-micron order imprinted light-guide plate (LGP) is proposed for edge-lit backlight unit. Optical characteristics of the imprinted LGP are examined by RCWA and the performance is verified through Monte Carlo simulation. Results show that the diffraction efficiency, luminous flux and its uniformity over the area are significantly affected by the angle of incident ray. Consequently couples of design considerations are additionally proposed to enhance luminous flux. In terms of peak luminance and out-coupling luminous flux, the experimental results are agreed well with the performance simulation. Finally, compared with optical characteristics of conventional backlight unit, we could conclude that the proposed simplified backlight unit made of diffractive grating imprinted light-guide plate is a good substitute for the conventional backlight unit.

Keywords : backlight, light-guide plate, diffractive grating, luminance enhancement, out-coupling flux, illumination, liquid crystal display

1. Introduction

Although an LCD occupies the predominant position among the flat panel display, since the liquid crystal itself is not an emissive device unlike OLED and PDP, there should be planar illuminator consisting of light sources and light guide optics beneath the LCD panel. This planar illuminator that is normally referred to as backlight unit in industry is classified into two groups, according to the location of light source; one is direct-lit backlight unit where several couples of light sources are placed behind the diffusive plate, and is usually adopted for LCD TV or high end monitor illumination and the other is edge-lit backlight unit where the light sources are placed at the edge of the guide plate for the illumination of notebook PC or small size mobile display. The typical edge-lit backlight unit is composed of two major parts, namely light source such as LED or cold cathode fluorescent lamp (CCFL) and backlight optics that includes a light-guide plate with printed dot patterns that scatter light into random direction, and a couple of prismatic sheets usually to enhance the luminance at normal direction and diffusers to hide the spotted appearance caused by dot patterned mask.

In order to achieve high luminance, several researches have been focused on modifying the surface of light-guide plate by employing micro optical structure instead of printed dots [1-4]. A. Horibe proposed a new concept LCD backlighting system using the highly scattering optical transmission (HSOT) polymer where spherical particles inside LGP function to extract the light [5-8]. Recently Y. Ishikawa developed the backlight for cellular phones with high intensified brightness upon the request of colored and higher pixel density displays [9]. In this report a high precision reflecting groove structure on the bottom of the light guide plate and a particular optical pattern imprinted on the top respectively were introduced to establish a new backlight technology with brighter output. As described above in order to increase the brightness and to reduce power consumption of an LCD panel, several approaches improving the light extraction performance and controlling the light directivity have been suggested. As a result of these new technologies, the upcoming edge-lit backlight unit is expected to be able to emanate more light than the conventional one in spite of the fewer components and slim size. However, it requires at least one downward-prismatic

Manuscript received December 6, 2003; accepted for publication March 8, 2004.

Corresponding Author : Hwan Young Choi
a. MEMS Lab., Samsung Advanced Institute of Technology, San 14-1, Nong-seo-ri, Kiheung-eup, Yong-in city, Kyungki-do, Korea.
b. Department of Mechanical Engineering, Yonsei University, 134 Shinchon-dong, Sudaemun-ku, Seoul 120-749, Korea.
E-mail : hychoi@samsung.com **Tel** : +31 280-9446 **Fax** : +31 280-9473

film to collimate the out-coupled and dispersed light from the light-guide plate because the light extracting principle of these recent light-guide plates for edge-lit backlight units still depends on light scattering and/or refraction,.

In this research, a highly simplified backlight unit mainly composed of diffractive grating imprinted LGP has been proposed, based on the diffraction characteristics of a surface relief grating with high spatial frequency. Since the incident light can be diffracted and coupled out from the LGP, the suggested BLU showed promising results to the extent of replacing prism sheets and still performing the light guide function at a satisfactory level [10-13]. The schematic structure is shown in Fig. 1(a) compared with conventional one depicted in Fig. 1(b). At the diffractive grating, incident beam acquires momentum, which is different for each wavelength and yet sufficient to over-come the condition of total internal reflection (TIR). Therefore, this study aims at not only optimizing the grating pattern but also providing additional design considerations for enhancing the light extraction efficiency by way of diffracting the light directly as much as possible toward the LCD panel.

2. Design of Diffractive Grating Imprinted LGP

The light out-coupling direction from the top of LGP through diffraction on surface-relief grating is a function of incident wavelength, incident angle, and the period of the grating. Assuming that the peak luminance could be determined based on the statistical behaviors of the incident rays, the grating period was determined to be 0.45 um based on the preliminary experiments where a peak luminance of normal direction was observed at 0.45 um [10]. From the grating equation, the representative incident angle is assumed to be 55°.

$$n_t \sin \theta_t - n_i \sin \theta_i = \frac{m\lambda}{\Lambda} \qquad (1)$$

2.1 Grating shape and depth

Since the out-coupling characteristics of imprinted LGP primarily depend on the diffraction characteristics of the highly frequent surface-relief grating pattern, we need to take into account diffraction efficiency in order to determine the grating depth and shape. By utilizing the rigorous coupled wave analysis method [14-16], the diffraction efficiency has been calculated with the condition of period 0.45 um and the chief incident angle as 55°. Fig. 2 shows the variation of diffraction efficiency of the grating for various shapes at 633 nm. In order for the diffraction efficiency to be robust against the positional shape variation in LGP, the range of grating depth should be narrowed to between 0.15~0.35 um, which minimizes the variation of diffraction efficiency in spite of the uneven shape. Fig. 3(a) shows the computational result of diffraction efficiency with 0.45 um period, sinusoidal grating for three different wavelengths and two polarization states at 55° of incidence. Optical properties of poly-methyl methacrylate (PMMA) were used for this simulation. Based on this result, almost the same diffraction

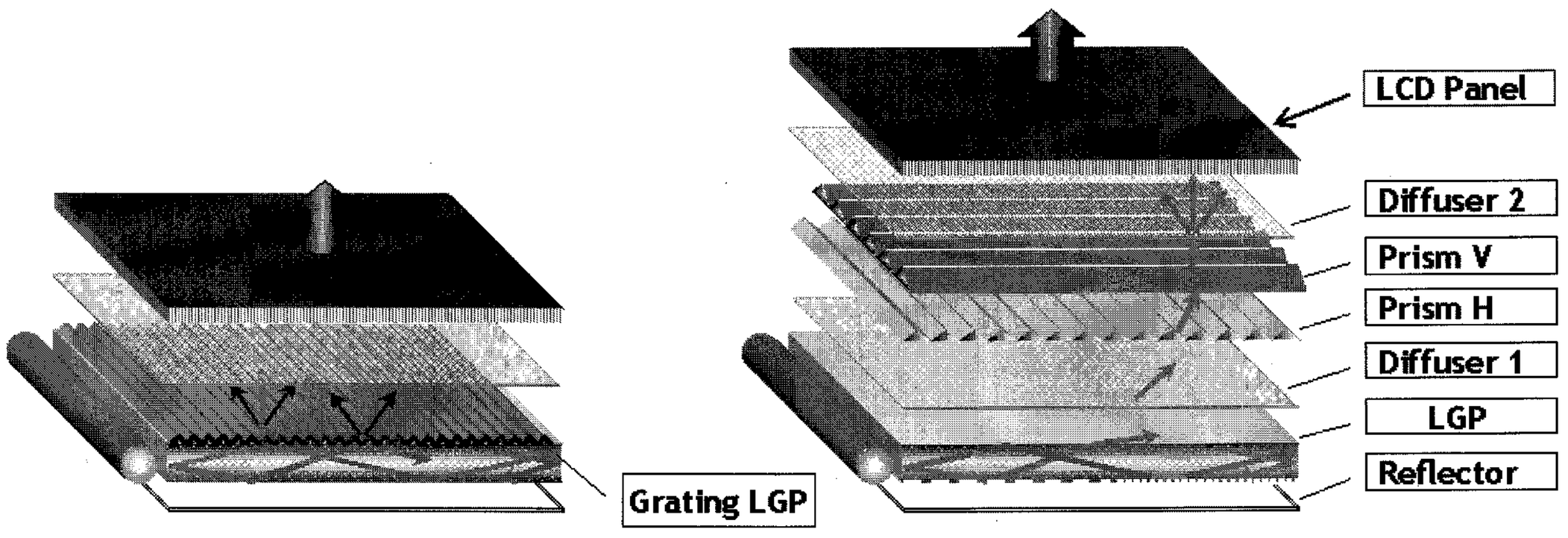

Fig. 1. Schematic diagram of edge-lit backlight unit (a) Diffractive grating imprinted light-guide plate. (b) Conventional light-guide plate where white spots or micro deflectors formed at the bottom.

efficiency in the range of visible light can be achieved at a grating depth ranging of between 0.15 um and 0.35 um. Fig. 3(b) shows the experimental result to examine the diffraction efficiency in real world. Comparing the two results, we found that the two are good agreement with each other when the depth is below 0.4 um. Figs. 4(a) and (b) show computational and experimental results of diffraction efficiency, respectively, when the incident angle varies from 40° to 90° for each wavelength and polarization. It should be noted that the efficiency of TE polarization for each wavelength is not meaningfully different with that of each other even though the computational result shows a slight difference in efficiency for each wavelength at the incident angle of around 50°.

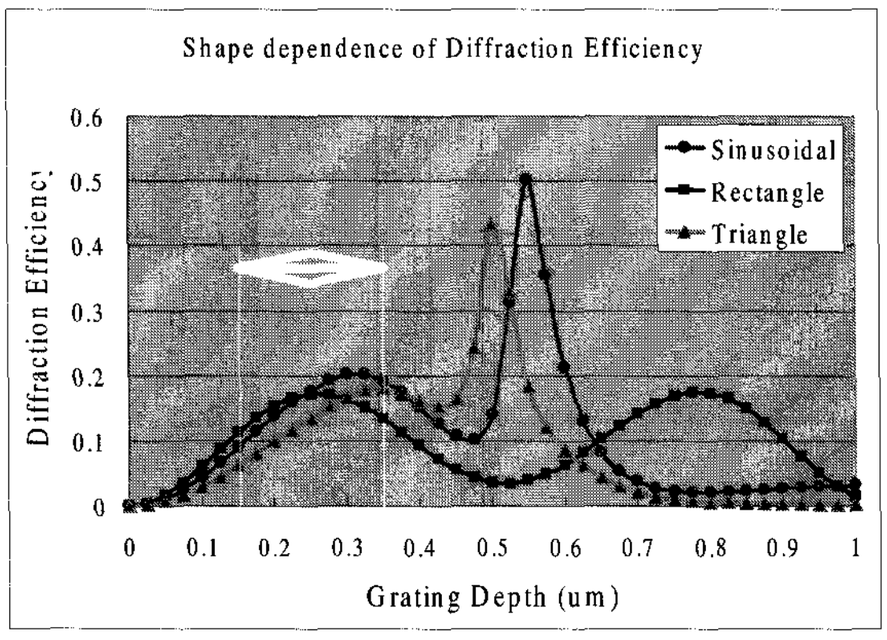

Fig. 2. Diffraction efficiency of three different grating shapes along with grating depth under the conditions of grating period 0.45 um, incident angle 55°, wavelength 633 nm and TE polarization.

2.2 Diffraction efficiency of transmission and reflection mode

Because the ray from the light source propagates into three dimensional spaces, the diffraction efficiency need to be calculated according to an arbitrary incident angle defined in terms of spherical coordinate (θ, ϕ) in Fig. 5. The ordinary light sources such as CCFLs and LEDs have a wide range of emitting angle; usually $0° \le \theta \le 90°$, $-90° \le \phi \le 90°$ and the peak luminous intensity at $\theta = 90°$, $\phi = 0°$. Through a simple calculation based on the following Snell's law, we found that the emitting angle varies due to refractive index difference between two materials as shown in Table 1.

$$n_1 \sin \theta_i - n_2 \sin \theta_t = 0 \qquad (2)$$

The refracted ray at the interface between air and PMMA exists under TIR (total internal reflection) condition which means that the incident angle normal to the surface is larger than the critical angle $\theta_c = 42.4°$. This implies that any light once injected into the rectangular hexahedral LGP structure can not be extracted, except the opposite facet of incidence, if there is neither an abnormal scattering nor extracting structure such as grating. As for each mode of transmission and reflection, the diffraction efficiency averaged over three wavelengths (460 nm, 540 nm, 620 nm) and two polarization states (TE & TM) was calculated and depicted in Figs. 6 and 7 respectively. As shown in Fig. 6, the diffraction efficiency of light greatly depends on the incident angle.

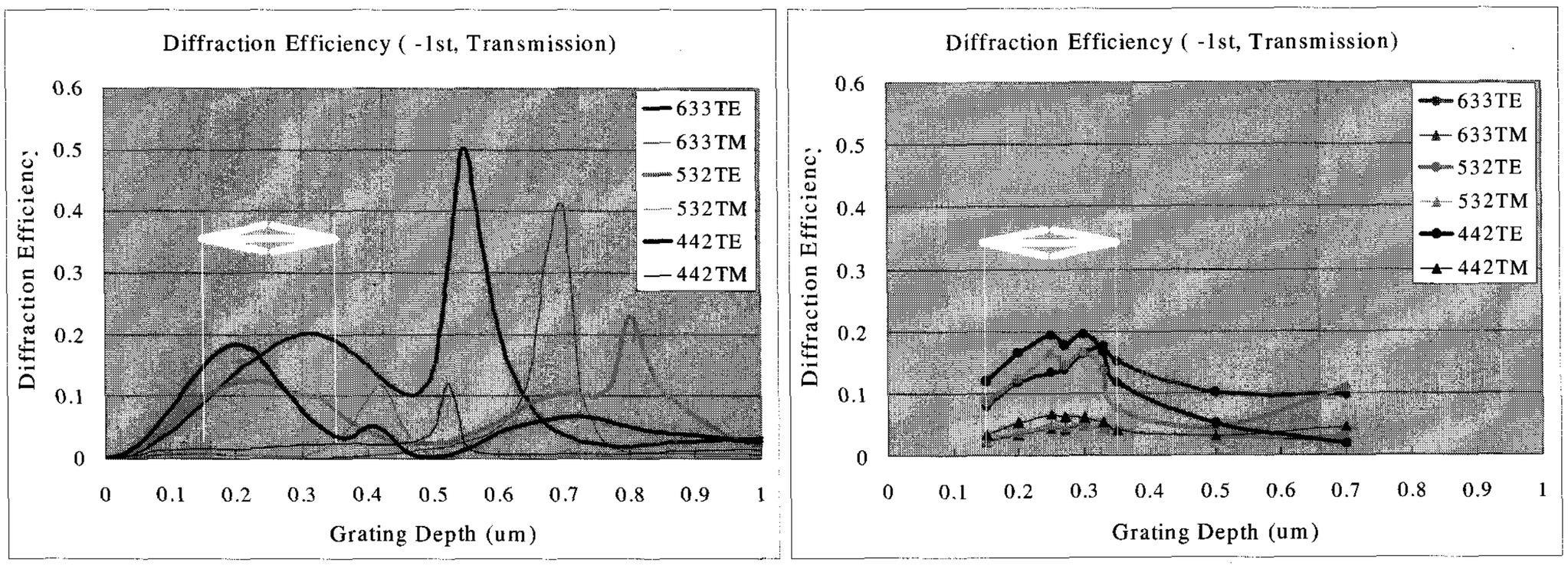

Fig. 3. Diffraction efficiency of sinusoidal shaped grating for each wavelength and TE, TM polarization depending on the grating depth (a) Numerical results; (b) Measured from pre-experiments (Grating period 0.45 um, incident angle 55°).

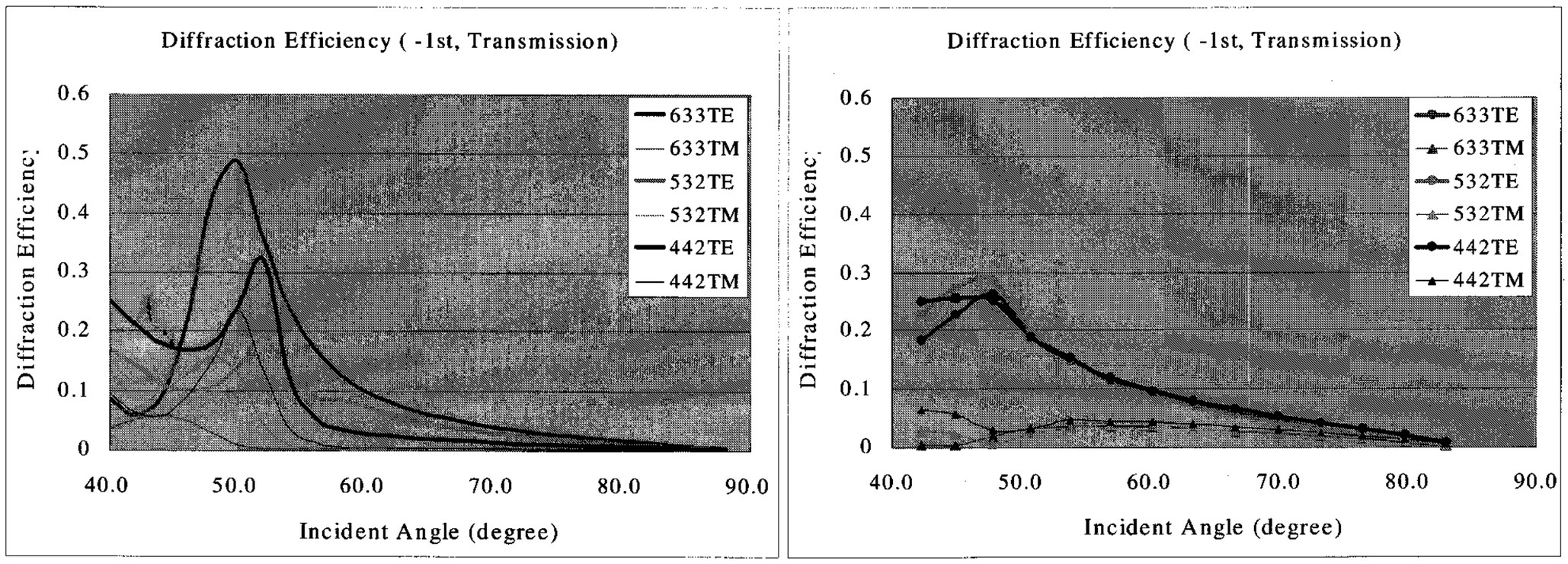

(a) (b)

Fig. 4. Diffraction efficiency of sinusoidal shaped grating for each wavelength and TE, TM polarization according to the incident angle: (a) Numerical results; (b) Measured data from pre-experiments (Grating period 0.45 um, depth 0.25 um).

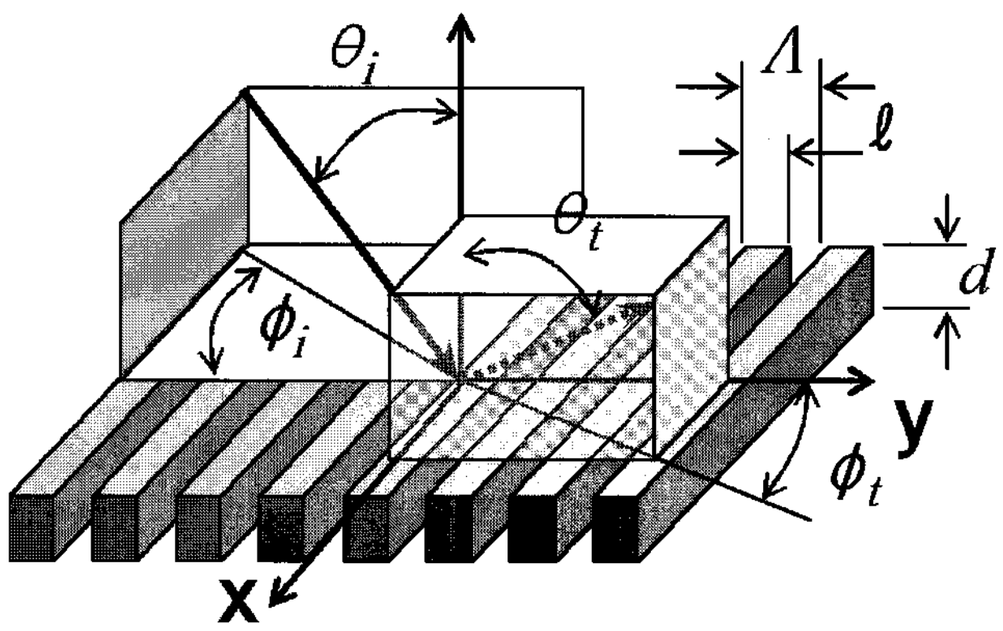

Fig. 5. Definition of incident and out-coupling angle in terms of Polar angle (θ) and Azimuth angle (ϕ).

Table 1. Emitting angle changes after the ray refracted inside the guide plate

Emitting angles	Incident ray ($n_1 = 1.0$)	Refracted ray ($n_2 = 1.492$)
Polar angle	$0° \le \theta \le 90°$	$47° \le \theta \le 90°$
Azimuth angle	$-90° \le \phi \le 90°$	$-47° \le \phi \le 47°$

The diffraction efficiency of transmission mode is 5 % to 15 % for $5° \le \theta \le 75°$, and there is no appreciable change in diffraction efficiency along ϕ for the given θ except the range $-55° \le \phi \le -20°$ and $20° \le \phi \le 55°$ where the efficiency reaches to 25 %. In case of reflection mode, the efficiency is higher than that of transmission. The peak diffraction efficiency and its corresponding incident angle

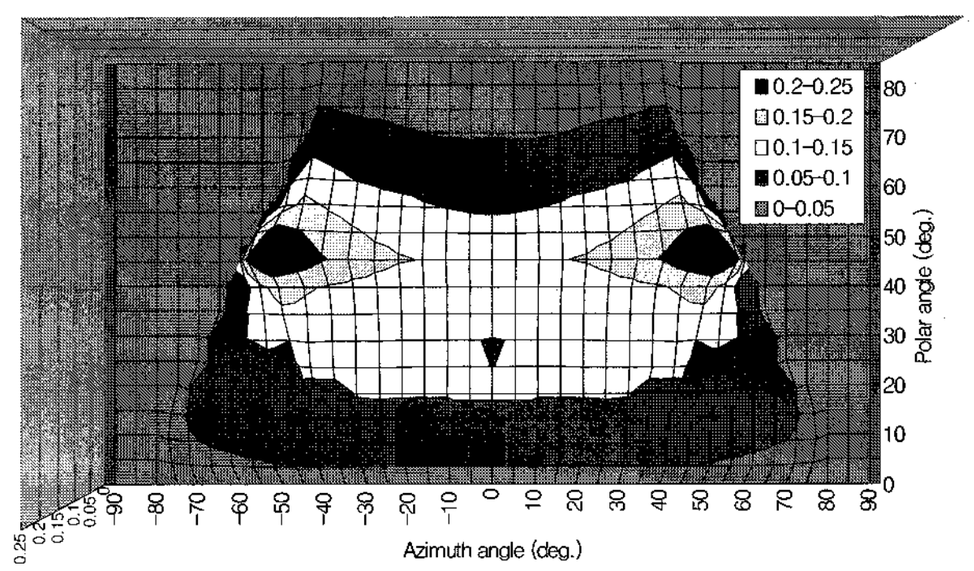

Fig. 6. Diffraction Efficiency of -1^{st} order transmission according to incident angle of θ and ϕ (Grating depth 0.25 um) averaged over 3 wavelengths (460 nm, 540 nm, 620 nm) and polarization state (TE & TM).

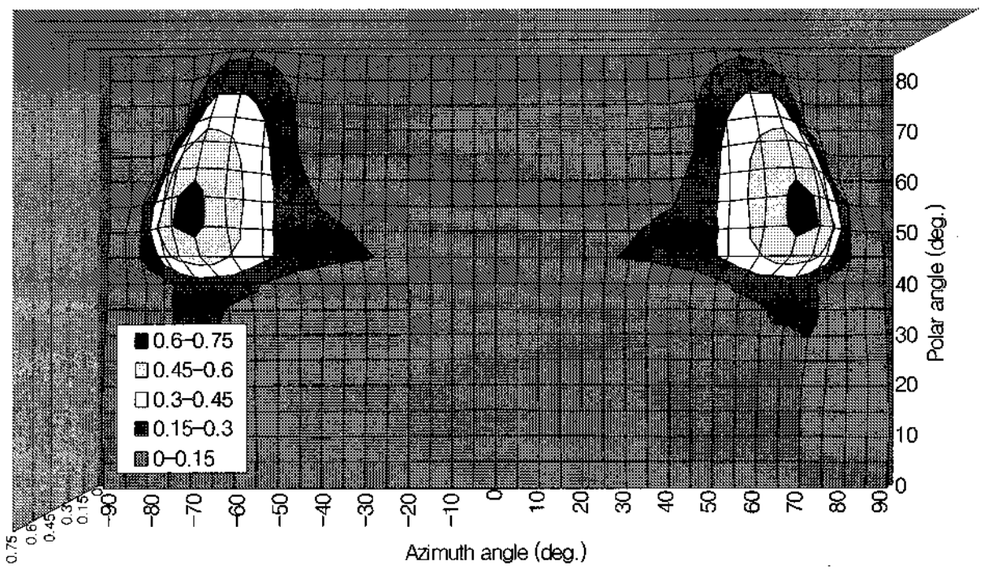

Fig. 7. Diffraction Efficiency of -1^{st} order reflection according to incident angle of θ and ϕ (Grating depth 0.25 um) averaged over 3 wavelengths (460 nm, 540 nm, 620 nm) and polarization state (TE & TM).

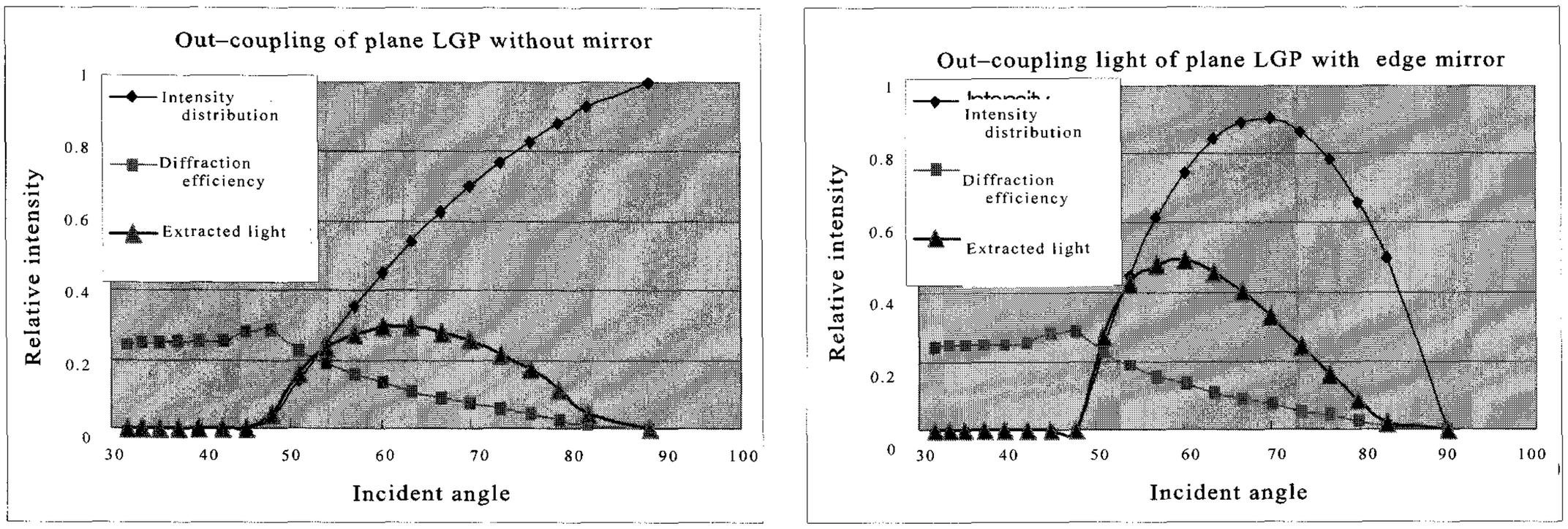

(a) (b)

Fig. 8. Relationship between extracted light amount and light source intensity distribution (a) in plane LGP without reflecting mirror and (b) in wedge-shaped or tapered edge mirror implemented LGP.

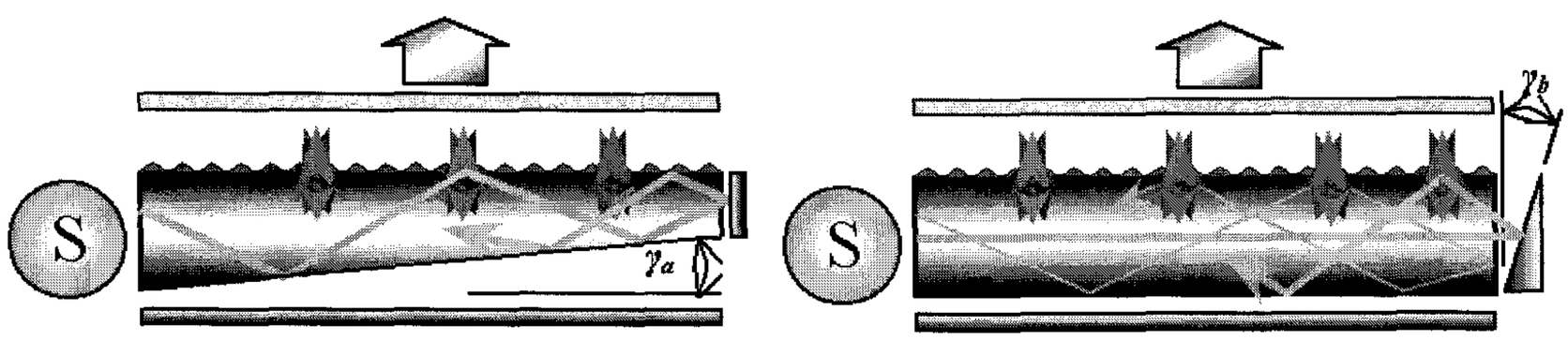

(a) (b)

Fig. 9. Polar angle change of peak luminous ray (a) Wedge-shaped light guide plate with plane reflection mirror in the end and (b) Flat plate with taper mirror.

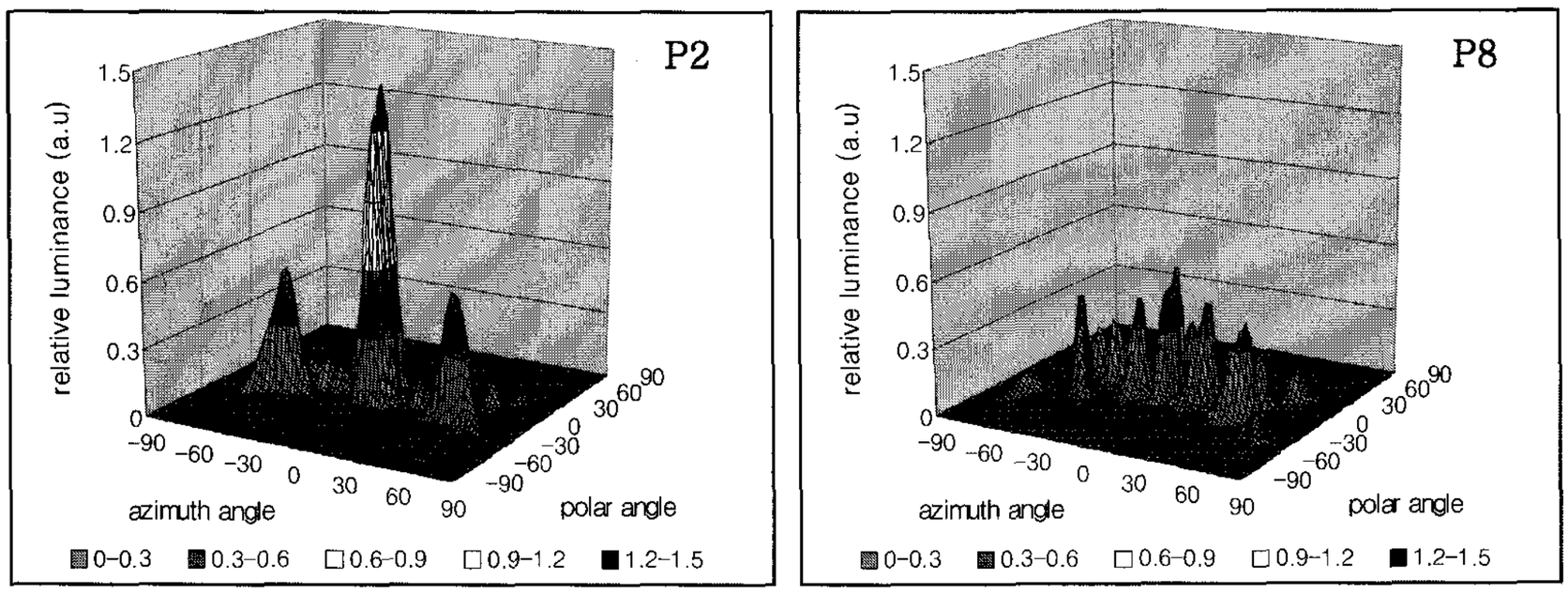

(a) (b)

Fig. 10. Luminance distribution of wedge-shaped LGP ($\gamma_a = 0.5°$) (a) near light source region P2 and (b) far region P8.

are shown in Fig. 6.

As shown in Fig. 6, the diffraction efficiency of -1st transmission becomes poorer as the polar angle θ increases to 90°, even though the incident ray has a peak intensity at the direction of $\theta = 90°$.

2.3 Out-coupling angle and simulation modeling

The diffraction efficiency calculated in Section 2.2 can be regarded as a diffraction probability density function **P** (θ_i, ϕ_i, m, λ: m is diffraction order) which represents the probability of diffraction mode for a given specific wavelength and incident angle. At the moment of diffraction, the ray propagation direction (θ_t, ϕ_t) is a function of its incident angle θ_i, ϕ_i, its wavelength λ, diffraction order m and polarization state. For any given θ_i, ϕ_i, m, ray propagation direction θ_t, ϕ_t after diffraction can be represented by following grating equation,

$$\cos\theta_t = \sqrt{1-(\frac{n_1}{n_2}\sin\theta_i\cos\phi_i+\frac{m\lambda}{n_2\Lambda})^2-(\frac{n_1}{n_2})^2\sin^2\theta_i\sin^2\phi_i}$$

$$\cos\phi_t = \frac{1}{\sin\theta_t}(\frac{n_1}{n_2}\sin\theta_i\cos\phi_i+\frac{m\lambda}{n_2\Lambda}) \qquad (3)$$

where n_1, n_2 are refractive indices before and after diffraction respectively. In this study, the polarization dependence is averaged for simplicity.

By utilizing Monte Carlo simulation with the probability density function and the out-coupling direction described in equation (3), the luminance distribution and out-coupling luminous flux in an arbitrary position of LGP can be represented as a summation of imaginary photons extracted from the plate.

2.4 Design considerations

Reminding that one of important functions of an LGP is how much and homogeneously extract the light from the plate so as to work as a planar illuminator for LCD, there is a strong need to change the light directivity inside the guide plate to be well accommodated with the gratings. As mentioned above the incident ray of $\theta = 90°$ hardly diffracts on the grating due to the very low diffraction efficiency in spite of peak incident intensity.

2.4.1 Polar angle correction to increase out-coupling energy

As shown in Fig. 8 in order to extract more light by diffraction it is necessary to alter the direction of peak luminous ray. It is a common problem occurs also in case of conventional system where white spots are printed on bottom of the plate to diffuse and extract the light. The typical solution for this problem is to make the plate wedge-shaped to change the direction gradually by the taper effect depicted in Fig. 9(a). Another solution is to place a tapered reflecting mirror in the end of the plate to change the direction of peak luminous ray described in Fig. 9(b).

Table 2 shows the number of photons per unit area (flux/m^2) emanating from the specified location of the LGP. The difference of averaged photon number between two types of θ correction method mentioned in Fig. 8 is not remarkable. However as depicted in Fig. 10, the luminance distribution along with the distance from lamp is significantly affected by the correction method. The peak luminance of P2 region which is near the light source (Fig. 10a) is three time higher than that of P8 region (Fig. 10b) in case of wedge-shaped LGP where as the difference of location is not serious in case of edge mirror placed LGP as shown in Fig. 11(a), (b). The difference causes non-homogeneous brightness which can not be acceptable.

2.4.2 Azimuth angle correction to enhance the luminance in normal direction

Another point of interest is the peak luminance in normal direction to LCD panel (practical luminance within viewing angle). In order to enhance the luminance in normal direction the out-coupling angle of extracted light needs to be within acceptable viewing angle. Therefore the out-coupling angle θ_t, ϕ_t should be as smaller as possible so that the emanating light can contribute to the normal luminance as much as possible.

Table 2. Photon density of specified region

Polar angle correction method	Photon density (flux/m^2)			
	P2	P5	P8	Mean
Wedge-shaped ($\gamma_a = 0.5°$)	1,668	1,244	1,202	1,371
Tapered edge mirror ($\gamma_b = 25°$)	1,646	1,314	1,453	1,471

Table 3. FWHM angle changes due to ϕ correction

ϕ correction	Plain LGP	Aerial lens	Side wall
FWHM(degree)	55°	28°	25°

However, the incident light of large azimuth angle of more than 30° also becomes the out-coupling light that has a large azimuth angle ϕ_t which hardly contributes to the luminance in the normal direction. And more the wide range of azimuth angle causes the un-homogeneous luminance distribution between the near light source region and far source region [13]. In the previous research, a two spherical surface lens carved inside the plate was proposed to restrict the azimuth angle within narrow limits. In this paper, however, another type of solution is suggested and investigated to confine the is azimuthally spreading. The FWHM angle

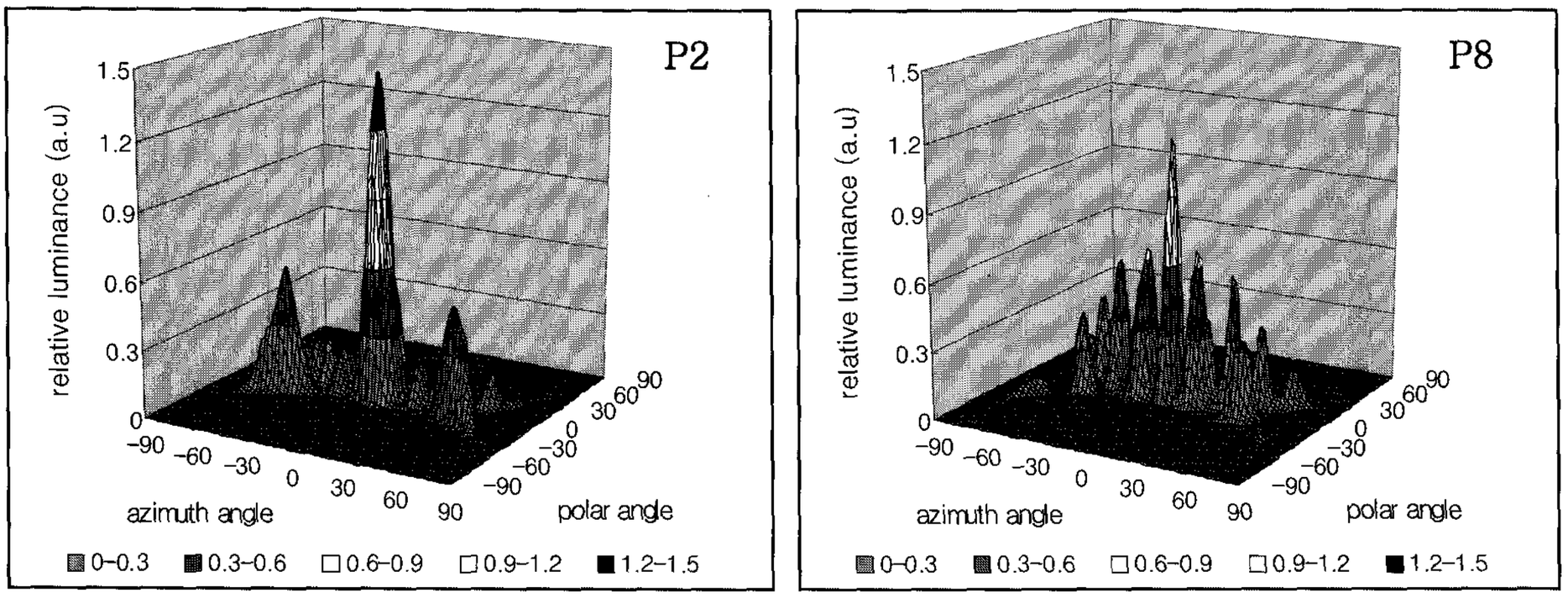

Fig. 11. Luminance distribution of taper mirror placed LGP ($\gamma_b = 25°$) (a) near light source region P2 and (b) far region P8.

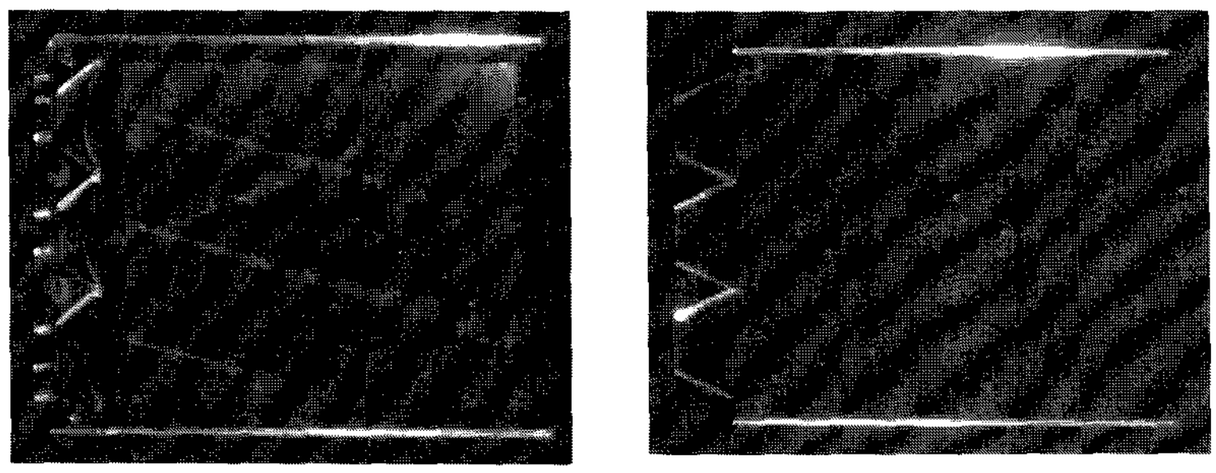

Fig. 12. Diffractive grating imprinted light-guide plate 1.8" diagonal size (a) aerial lens carved and (b) side wall implemented.

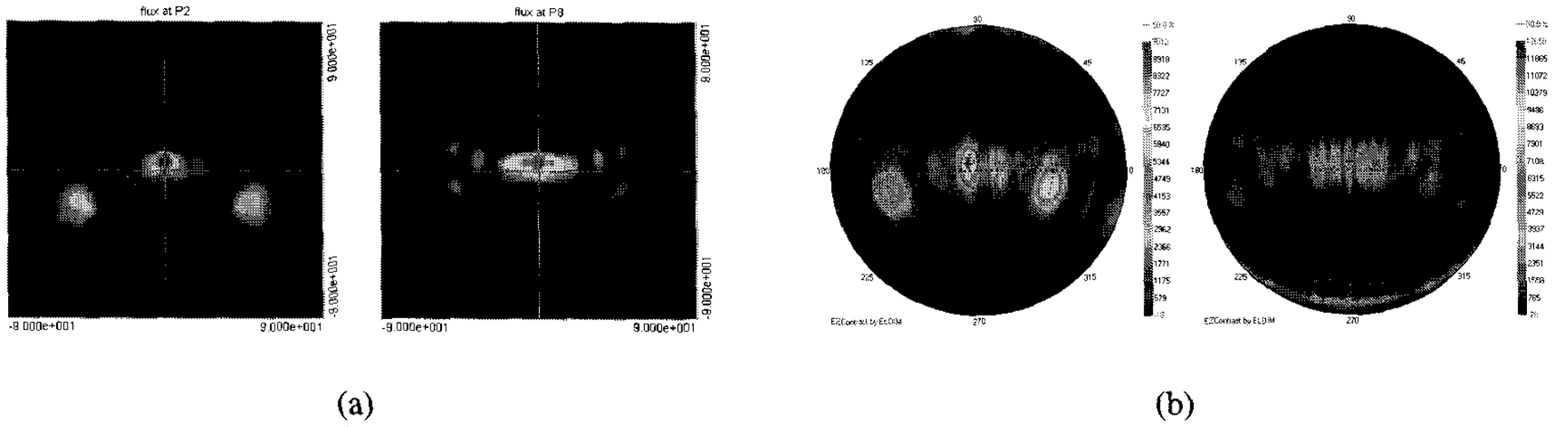

Fig. 13. (a) Computed luminance distribution at P2, P8 and (b) measured distribution of imprinted light-guide plate.

for each type is described in Table 3.

Table 4 shows the quantity of photons counted over the region specified above for each ϕ correction implemented. According to the simulation results, the average out-coupling photon number of LGP where aerial lens has been carved inside is much fewer than those of plain LGP. It is assumed that it was caused by the aerial lens that diminishes the light flux when it transverse the surface.

Table 4. Photon density depending on ϕ correction method

Azimuth angle correction method	Photon density (flux/m^2)			
	P2	P5	P8	Mean
Plain LGP	1,646	1,314	1,453	1,471
Aerial lens LGP	1,192	935	1,078	1,068
Side wall LGP	2,008	1,357	1,666	1,677

3. Experiments

At the design stage, the dimension of diffractive grating was set as Λ = 0.45 um and d = 0.25 um. Since the period of grating is beyond the mechanical tooling, interference lithography was adopted for generating the fine patterns on glass substrate. Then, the sub-micron structures were replicated on two types of PMMA plates where the azimuth correction means had been implemented beforehand. Replication was performed mainly using UV-curable resin and the diffraction efficiency was measured to confirm that the patterns have been transferred properly. Fig. 12 shows the diffractive grating imprinted light-guide plates where the aerial lens carved inside the plate (a) and side wall implemented (b).

4. Results and Discussions

As shown in Figs. 13(a) and (b), in both case of

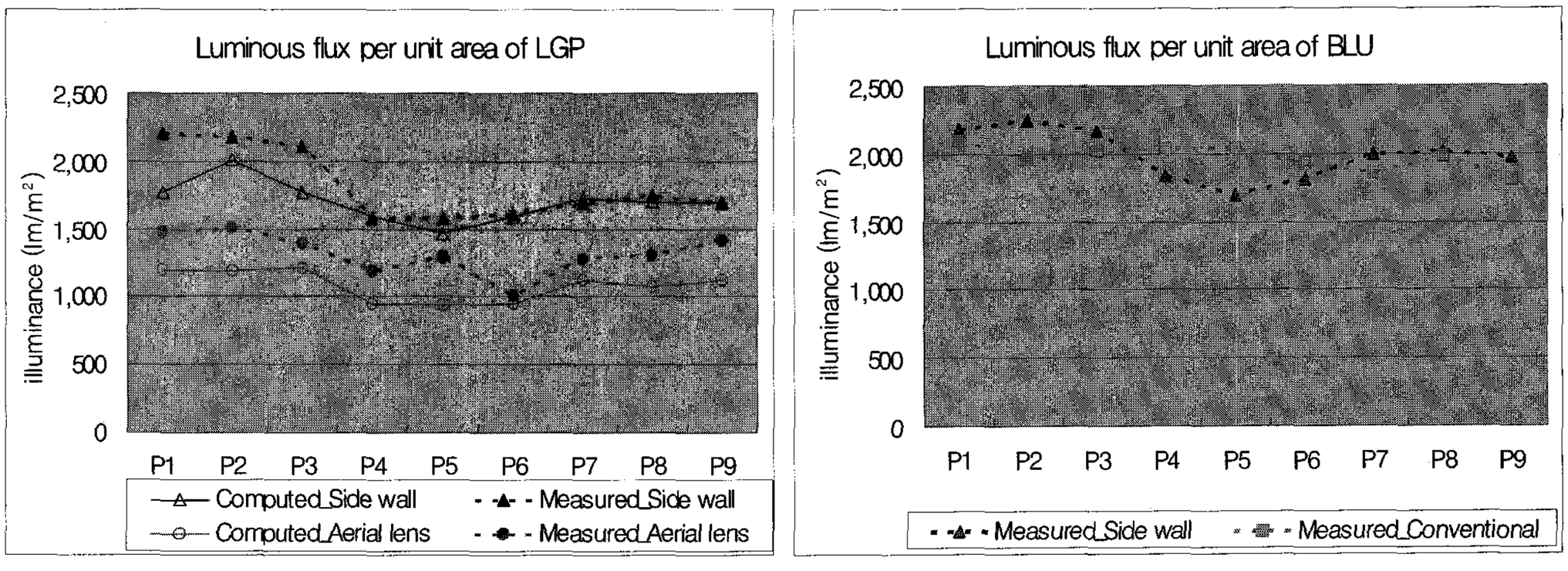

Fig. 14. (a) Measured and computed luminous flux density of aerial lens and side wall type LGP and (b) measured luminous flux density of the conventional BLU and simplified BLU.

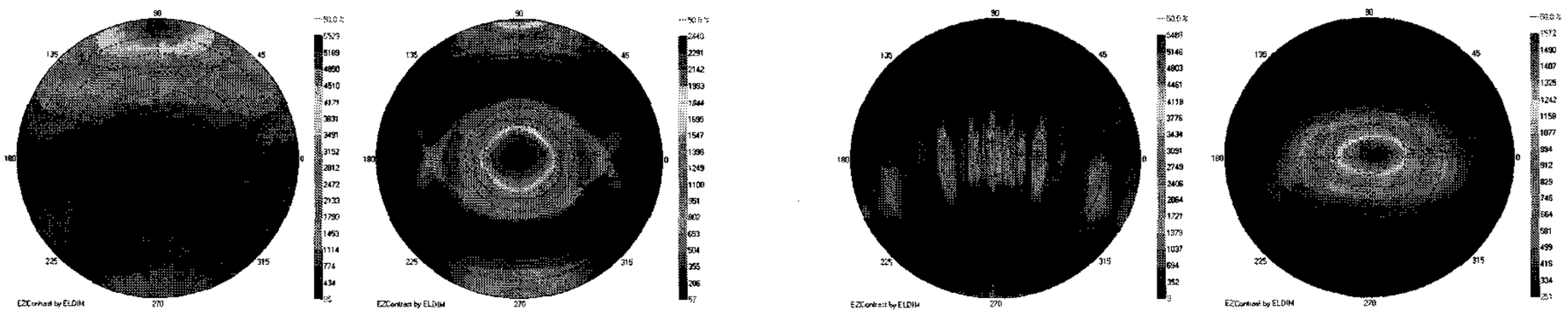

Fig. 15. Luminance angular distribution of (a) conventional LGP and BLU and (b) grating imprinted LGP and assembled BLU.

computed and experimented luminance distribution of imprinted LGP at P2 and P8 region, the peak luminance is observed to be at normal direction ($\theta t = 0°$, $\phi t = 0°$) which means that the incident rays were diffracted and out-coupled by the grating imprinted on the surface of LGP, even though there was a slight difference in luminance distribution between P2 and P8 region. The computed result showed that it is in good agreement with that of the experiment. To investigate the performances of imprinted LGP, the angular luminance distribution and luminous flux were measured by ELDIM EZContrast 160^{TM} along with the designated nine regions. As shown in Fig. 14(a), in terms of out-coupling luminance flux, the side wall implemented LGP is superior to aerial lens type as forecast by computation. This suggests that the out-coupling flux in experiments is more than expected by the computation in both case of side wall and aerial lens type LGP. We assume that there is another out-coupling path that has been neglected in computation for simplification. Finally, luminous flux of imprinted LGP with a diffuser on top is compared with that of conventional BLU as shown in Fig. 14(b). It can be seen that the out-coupling flux over the entire area of the conventional BLU is more homogeneous than that of imprinted LGP with a diffuser. However, at the point of total out-coupling flux no significant difference can be observed between the conventional and proposed BLU.

Fig. 15 shows a luminance angular distribution of conventional LGP and BLU (a), in comparison with grating imprinted LGP and BLU (b). There appear to be no unnecessary luminance distribution caused by large angle out-coupling which can be found in conventional BLU as shown on the right-hand side of Fig. 14 (a).

5. Conclusions

Following the worldwide research trend on next generation backlight unit development, simplified backlight unit mainly composed of diffractive grating in sub-micron order imprinted LGP has been proposed for edge-lit backlight unit. The optical characteristics of grating imprinted LGP were analyzed in terms of diffraction efficiency and out-coupling energy per unit area. Consequently, couples of design considerations were suggested to maximize peak luminance and out-coupling energy. Through the computational simulation and prototyped samples, we conclude the following.

1) As for the incident angle correction, the side wall implemented LGP shows better performance than the aerial lens type

2) For both cases of azimuth angle corrected LGP, the performance is significantly affected by the tapered mirror placed to alter the peak intensity ray toward the representative angle direction

3) From the comparison between the performances of prototyped samples and conventional ones, the newly proposed light-guide plate is expected to be a good candidate for next generation backlight unit.

References

[1] Y. Oki, in SID 98 Digest (1998), p. 157.

[2] K. Kalantar, in SID 99 Digest (1999), p. 764.

[3] K. Kalantar, S. Matsumoto, T. Onishi, and K. Takizawa, in SID 00 Digest (2000), p. 1029.

[4] T. Ide, H. Numata, H. Mizuta, Y. Taira, M. Suzuki, M. Noguchi, and Y. Katsu, in SID 02 Digest (2002), p. 1232.

[5] A. Horibe, M. Bada, E. Nihei, and Y. Koike, in SID 98 Digest (1998), p. 153.

[6] A. Tagaya, M. Nagai, Y. Koike, and K. Yokoyama, Applied Optics, **40**, 6274 (2001).

[7] A. Tagaya, S. Ishii, K. Yokoyama, E. Higuchi, and Y. Koike, Jpn. J. Appl. Phys. **41**, 2241 (2002).

[8] H. Suzuki, M. Horiguchi, T. Okumura, A. Tagaya, and Y. Koike, in Proceeding Asia Display / IDW '03 (2003), p. 673.

[9] Y. Ishikawa, Hitachi Chemical Technical Report **42**, 39 (2004) in Japanese

[10] H. Y. Choi, M. G. Lee, J. H. Min, and J. S. Choi, in Proceeding Asia Display / IDW '01 (2001), p. 521.

[11] M. G. Lee, H. Y. Choi, J. H. Min, J. S. Choi, J. H. Kim, and S. M. Lee, in Proceeding EURO Display (2002), p. 343.

[12] S. M. Lee, H. Y. Choi, M. G. Lee, J. H. Min, J. S. Choi, J. H. Kim, S. I. Kim, Y. S. Choi, and K. H. Lee, in SID 03 Digest (2003), p. 1361.

[13] J. H. Min, H. Y. Choi, M. G. Lee, J. S. Choi, J. H. Kim, and S. M. Lee, Journal of the SID **11**, 653 (2003).

[14] M. G. Moharam, Eric B. Grann, Drew A. Pommet, and T. K. Gaylord, J. Opt. Soc. Am. A **12**, 1068 (1995).

[15] P. Lalanne and G. Michael Morris, J. Opt. Soc. Am. A **13**, 779 (1996).

[16] S. Peng and G. Michael Morris, J. Opt. Soc. Am. A **12**, 1087 (1995).